Sensitivity analysis of viscoelastic full waveform inversion

Shahpoor Moradi* and Kris Innanen

*moradis@ucalgary.ca

Introduction

Fréchet kernels for FWI of multicomponent data for a linear isotropic viscoelastic media are derived by using the Born approximation applied to the Green's integral solution of the wave equation. The kernels that also called scattering potentials are the functions of opening angle between the incident and scattered waves and attenuation angle that characterized the maximum direction of the attenuation. Sensitivities of the full recorded viscoelastic wave-field are obtained in three types of model parametrization, density-velocity-quality factor, $[\rho, V_P, V_S, Q_P, Q_S]$, density-impedance quality factor $[\rho, Z_P, Z_S, Q_P, Q_S]$, and density-Lamé parameter -quality factor, $[\rho, \lambda, \mu, Q_P, Q_S]$. We also study the radiation patterns of point sources and moment tensor sources, among them, a dipole and double couple sources in a viscoelastic medium, this analysis can be used for the inversion of the seismic sources in an attenuative medium.

Source radiation pattern in viscoelastic media

The viscoelastic wave is characterized by a complex wavevector whose real part is the propagation vector and imaginary part is attenuation vector. A wave with nuparallel propagation and attenuation vectors is called inhomogeneous otherwise called homogenous. Due to complexity of the wavenumber vector, polarization and slowness vectors are complex.

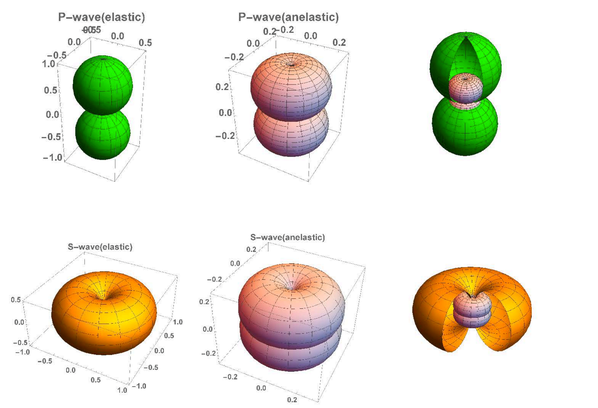

Figure 1: Diagram illustrating the 3-dimensional radiation patterns generated by a point source in z direction for P- and S-waves. The top left figure is the real part of the radiation pattern of the source for P-wave, the higher lobe is due to the force in the positive z-direction and lower lobe is due to the point force in negative z-direction. The top middle figure is the imaginary part of the radiation pattern for P-wave in a different scale comparing to the real part. Top right is a figure that compares the real and imaginary parts of the radiation patterns. The same interpretation for the radiation patterns for S-wave.

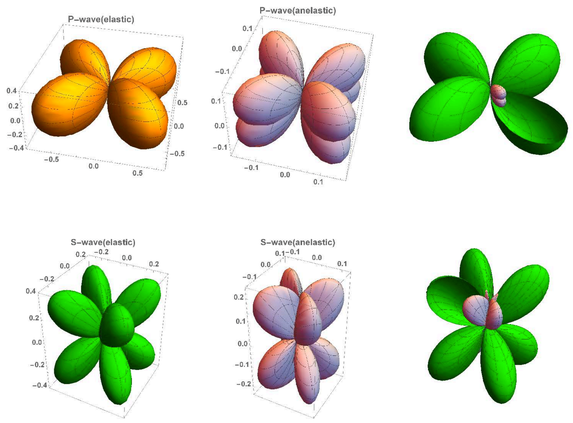

Figure 2: Diagram illustrating the 3-dimensional radiation patterns generated by a double couple M_{xy} for P- and SI-waves. Format and interpretation are the same as fig. 1.

Born approximation

The essence of derivation of scattering potentials is based on the Born approximation which deals with the first order scattering.

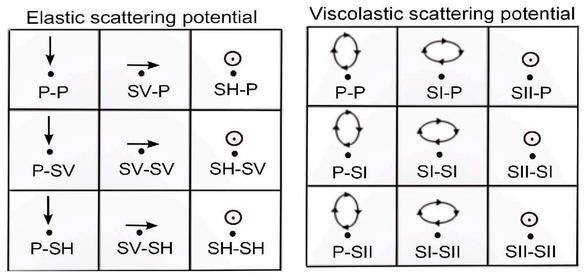

Figure 3: Left figure illustrates the components of scattering potential for scattering from elastic perturbations. Arrows indicate the polarization of the incident waves, P-, SV, and SH-waves have linear polarizations. Right figure illustrates the components of scattering potential for scattering from elastic and anelastic perturbations. Polarization for P- and SI-waves is elliptical whereas for SII-wave is linear.

Sensitivity of the viscoelastic wave-field data

Table 1: P-P sensitivities: density-velocity

	Perturbation	Sensitivity
Elastic	density	$-1-\cos\sigma_{PP}+2\left(\frac{V_{SE}}{V_{PE}}\right)^2\sin^2\sigma_{PP}$
	P-wave velocity	-2
	S-wave velocity	$4\left(\frac{V_{SE}}{V_{PE}}\right)^2\sin^2\sigma_{PP}$
Anelastic-homogeneous	density	$2(Q_S^{-1}-Q_P^{-1})\left(\frac{V_{SE}}{V_{PE}}\right)^2\sin^2\sigma_{PP}$
	P-wave velocity	0
	S-wave velocity	$4(Q_S^{-1}-Q_P^{-1})\left(\frac{V_{SE}}{V_{PE}}\right)^2\sin^2\sigma_{PP}$
	P quality factor	Q_P^{-1}
	S quality factor	$-2Q_S^{-1}\left(\frac{V_{SE}}{V_{PE}}\right)^2\sin^2\sigma_{PP}$
Anelastic-inhomogeneous	density	$Q_P^{-1}\tan\delta_P\left[\sin\sigma_{PP}+2\left(\frac{V_{SE}}{V_{PE}}\right)^2\sin 2\sigma_{PP}\right]$
	P-wave velocity	0
	S-wave velocity	$4Q_P^{-1}\tan\delta_P\left(\frac{V_{SE}}{V_{PE}}\right)^2\sin 2\sigma_{PP}$

Table .1 describes all components of the sensitivities for elastic, anelastic-homogeneous and anelastic-inhomogeneous terms.

$\Delta\rho\neq 0,\quad \mathbb{V}^{\rho}_{E}(\Delta V_{PE},\Delta V_{SE})$

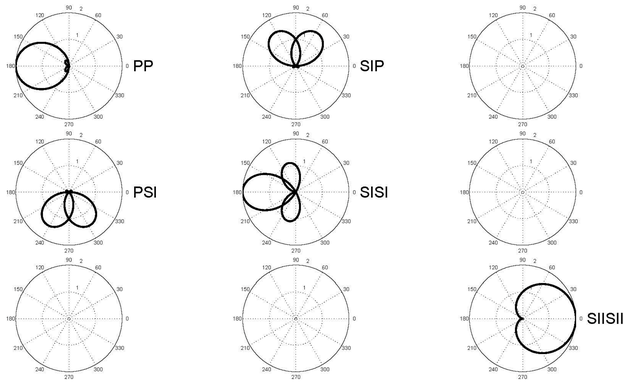

Figure 4: Elastic part of viscoelastic sensitivity matrix parameterized by (ρ, V_{SE}, V_{PE}) for density diffractor for the five scattering modes P-P, P-SI, SI-P, SI-SI and SII-SII. These patterns are the same with elastic scattering modes P-P, P-SV, SV-P, SV-SV and SH-SH. The patterns are plotted as a function of the opening angle. Sensitivities are derived in the context of Born approximation.

Linearized scattering matrix continued

$\Delta\rho\neq 0,\quad \mathbb{V}^{\rho}_{HM}(\Delta V_{PE},\Delta V_{SE})$

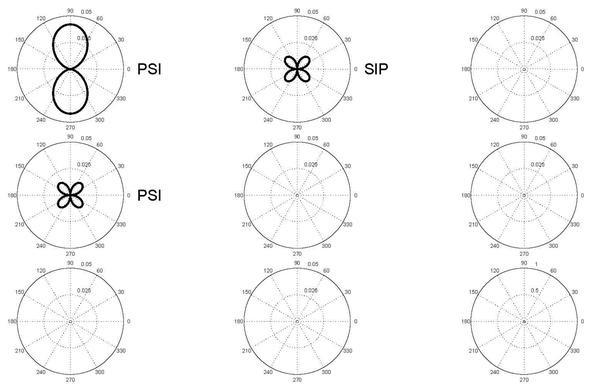

Figure 5: Anelastic-homogenous part of viscoelastic sensitivity matrix parameterized by (ρ, V_{SE}, V_{PE}) for density diffractor.

$\Delta\rho\neq 0,\quad \mathbb{V}^{\rho}_{IHM}(\Delta V_{PE},\Delta V_{SE})$

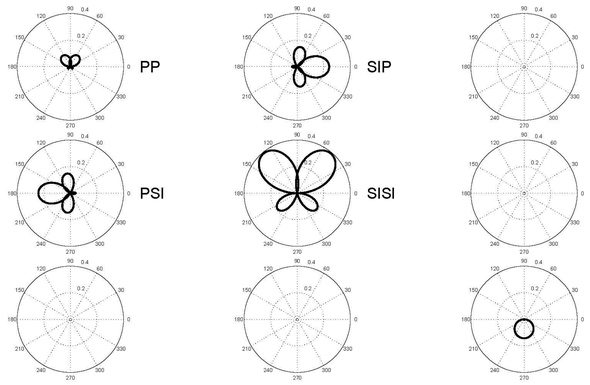

Figure 6: Anelastic-inhomogenous part of viscoelastic sensitivity matrix parameterized by (ρ, V_{SE}, V_{PE}) for density diffractor for the five scattering modes P-P, P-SI, SI-P, SI-SI and SII-SII.

Conclusions

In conclusion in this research we study the sensitivity of the full waveform inversion to the changes in five viscoelastic parameters. We examine our theory in three types of model parametrization, namely, density-velocity-quality factor, density-impedance-quality factor and density-Lame parameter-quality factor. To obtain the sensitivities we used the single scattering approximation called Born approximation. We also investigate the effects of anelasticity on the source radiation patterns for three types of sources: point source, dipole source and double couple source.

Acknowledgment

The authors thank the sponsors of CREWES for continued support. This work was funded by CREWES industrial sponsors and NSERC (Natural Science and Engineering Research Council of Canada) through the grant CRDPJ 461179-13.

Bibliography

Please see the report for references.